Experimental Measurement of Noncovalent Interactions Between Halogens and Aromatic Rings

Harry Adams,[a] Scott L. Cockroft,[a] Claudio Guardigli,[a] Christopher A. Hunter,*[a] Kevin R. Lawson,[b] Julie Perkins,[a] Sharon E. Spey,[a] Christopher J. Urch,[b] and Rhonan Ford[c]

Chemical double mutant cycles have been used to quantify the interactions of halogens with the faces of aromatic rings in chloroform. The halogens are forced over the face of an aromatic ring by an array of hydrogen-bonding interactions that lock the complexes in a single, well-defined conformation. These interactions can also be engineered into the crystal structures of simpler model compounds, but experiments in solution show that the halogen–aromatic interactions observed in the solid state are all unfavourable, regardless of whether the aromatic rings contain electron-withdrawing or electron-donating substituents. The halogen–aromatic interactions are repulsive by 1–3 kJ mol^{-1}. The interactions with fluorine are slightly less favourable than with chlorine and bromine.

Introduction

Noncovalent interactions involving halogens have been a matter of debate in the literature for many years.[1] As expected for electronegative elements with accessible lone pairs, halogens can act as hydrogen-bond acceptors, but in the 1950s, it became clear that halogens could also form complexes with hydrogen-bond acceptors.[2] This behaviour has been rationalised based on molecular electrostatic potential surfaces (Figure 1).[3] Fluorine behaves like a ball of negative charge, so that it can only act as a hydrogen-bond acceptor. The other halogens have a more positive region on the surface opposite to the X–C bond direction as well as an equatorial belt of negative potential, so that they can act as hydrogen-bond donors or acceptors depending on the angle of approach. The magnitude and area of the zone of positive potential increases with the size of the halogen, so that iodine in particular makes relatively strong interactions with hydrogen-bond acceptors. This view is borne out by an analysis of the geometric preferences of the interactions of hydrogen-bond donors and acceptors with halogens in the Cambridge Structural Database.[4]

Noncovalent interactions between halogens and aromatic rings were first discussed in relation to the so-called charge-transfer complexes formed between molecular iodine and aromatics such as mesitylene.[5] However, halogen–π interactions are not commonly observed, and the possible role of such interactions in more complicated molecular recognition events is not clear. Ooki has used a triptycene torsion balance to compare the interactions of a methyl group and a chloro group with substituted aromatic rings.[6] Aromatics with electron-withdrawing substituents preferred to interact with the chloro group, but all other aromatics preferred to interact with the methyl group. However, the details of the interaction geometries are not known.

In this paper, we report a systematic study of the thermodynamic properties of the halogen–π interaction as a function of the identity of the halogen and substituents on the aromatic ring. The approach is based on the chemical double mutant cycle method that we have developed for measuring weak intermolecular interactions within synthetic hydrogen-bonded complexes in chloroform.[7] The approach is illustrated for the previously reported measurement of aromatic interactions in Figure 2. To quantify the terminal aromatic interaction in complex A, we can compare the free energy of complexation of

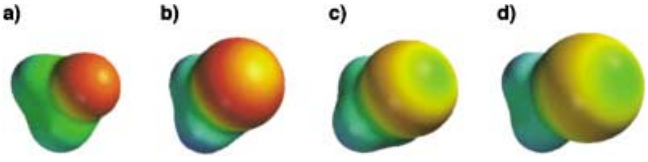

Figure 1. *Molecular electrostatic potential surfaces of (a) methyl fluoride, (b) methyl chloride, (c) methyl bromide and (d) methyl iodide calculated by using the STO-3G basis set in Spartan. The red regions represent negative electrostatic potential, the blue regions positive electrostatic potential, and yellow is neutral.*

[a] *H. Adams, S. L. Cockroft, C. Guardigli, Prof. C. A. Hunter, J. Perkins, S. E. Spey*
Centre for Chemical Biology, Krebs Institute for Biomolecular Science
Department of Chemistry, University of Sheffield
Sheffield, S3 7HF (UK)
Fax: (+44) 114-273-8673
E-mail: c.hunter@sheffield.ac.uk

[b] *Dr. K. R. Lawson, Dr. C. J. Urch*
Zeneca Agrochemicals
Jealott's Hill Research Station
Bracknell, RG42 6ET (UK)

[c] *Dr. R. Ford*
AstraZeneca Charnwood
Bakewell Road, Loughborough, LE11 5RH (UK)

 DOI: 10.1002/cbic.200400018

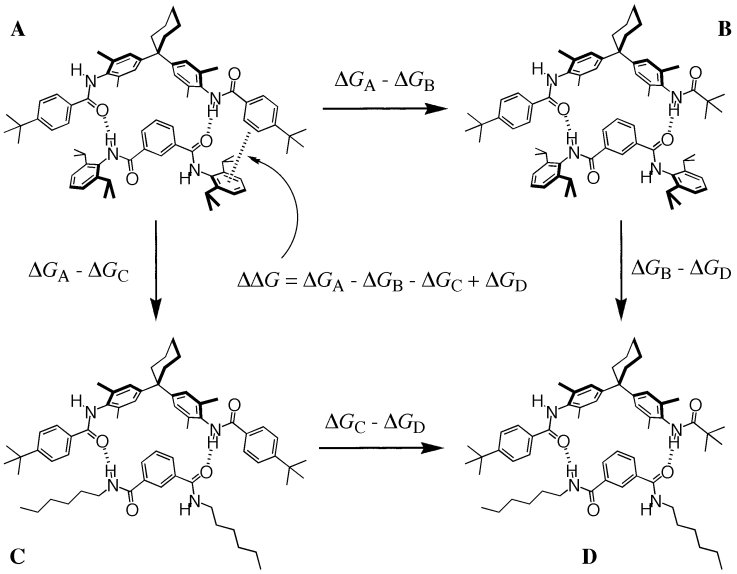

Figure 2. *Chemical double mutant cycle to measure the terminal edge-to-face aromatic interaction in complex A.*

complex A with either complex B or complex C. In both cases, one of the interacting aromatic rings is missing, and so $\Delta G_A - \Delta G_B$ or $\Delta G_A - \Delta G_C$ provides an estimate of the free energy contribution of the aromatic interaction to complex A. However, this simplistic analysis does not allow for any changes in hydrogen bond strength or secondary interactions involving the aromatic ring that is removed. These additional contributions can be measured by using the double mutant, complex D. Thus, the difference $\Delta G_C - \Delta G_D$ provides a direct measure of any secondary effects that contribute to the difference $\Delta G_A - \Delta G_B$, and hence allows us to dissect out the free energy contribution of the terminal aromatic interaction from all of the other interactions present in complex A [Eq. (1)]:

$$\Delta\Delta G = \Delta G_A - \Delta G_B - \Delta G_C + \Delta G_D \quad (1)$$

Here, we show how this system can be adapted to quantify halogen–aromatic interactions.

Results and Discussion

Design and synthesis

X-ray crystal structures of simple model compounds can be used to probe the geometry of the terminal interaction of complex A in Figure 2. Thus, **3** forms a hydrogen-bonded polymer with the head-to-tail packing and the same edge-to-face aromatic interactions that are present in the **1·2** complex in solution (Figure 3).[8] It is important to note that the complexes are not symmetric. At one end, the benzoyl carbonyl oxygen atom is a hydrogen-bond acceptor, and at the other, the benzoyl amide moiety is a hydrogen-bond donor. Consequently, there are two different geometries of interaction between the terminal functional groups, designated α and β in Figure 3. The two different interaction geometries are also found in the X-ray crystal structures of the model compounds (Figure 3). To investigate the possibility of introducing halogen–aromatic interactions into this system, twelve model compounds (**4**–**15**) were prepared by coupling tribromoacetyl chloride, trichloroacetyl chloride, trifluoroacetic anhydride or acetic anhydride with three 2,6-diisopropylaniline derivatives (Scheme 1). Single-crystal X-ray structures were ob-

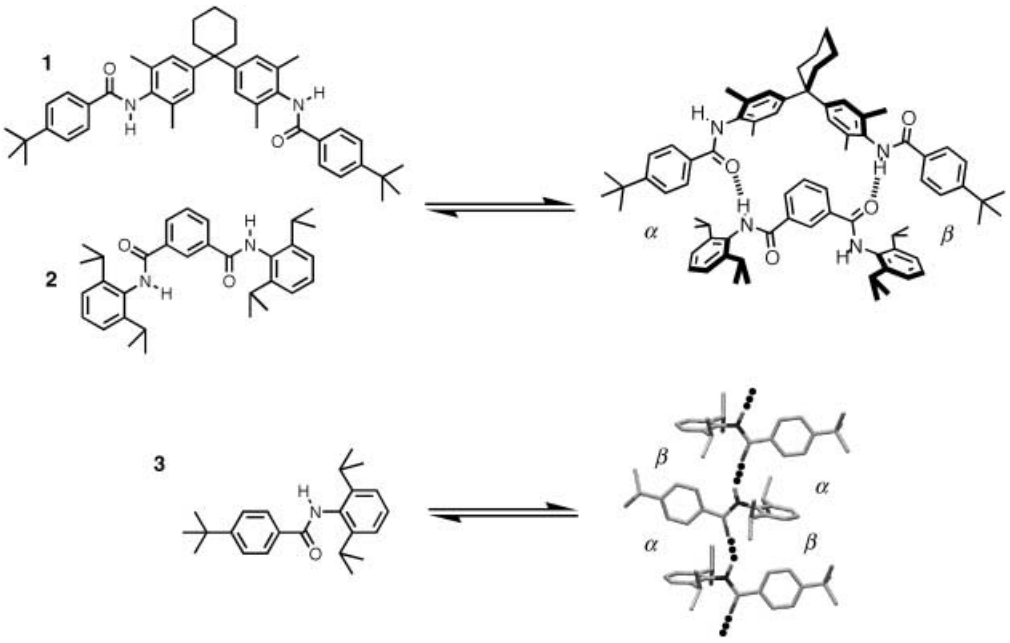

Figure 3. *The **1·2** zipper complex used to measure the terminal edge-to-face aromatic interaction in solution, and model compound **3** used to probe the geometry of this interaction in the solid state. Three molecules from the X-ray crystal structure of **3** are shown. The α and β interaction geometries are labelled.*

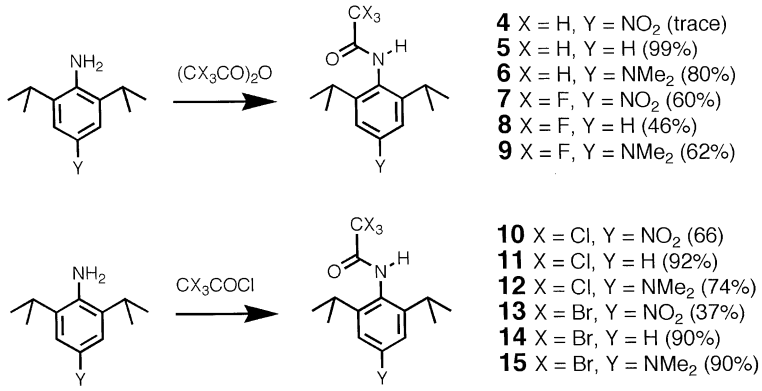

Scheme 1. *Preparation of model compounds **4**–**15** by direct trihaloacetylation or acetylation of 2,6-diisopropylanilines.*

tained for nine of these compounds. The packing of the molecules in the solid state is remarkably similar in all of the crystal structures (Figure 4). The molecules are arranged in hydrogen-bonded chains in a head-to-tail orientation with the CX_3 groups over the faces of the aniline π systems. The shortest halogen–aromatic contact occurs for the α geometry interaction (Figures 4 and 5). One of the halogens is in van der Waals contact with the aromatic ring in all of the structures, and the angle (ϕ) between the C–X bond and the plane of the π system is 20–40° away from orthogonal (Table 1). It might be tempting to ascribe this observation to attractive interactions between the CX_3 groups and the aromatic rings, but as will become clear this is not the case.

In all of the X-ray crystal structures of the model compounds, the shortest halogen–aromatic contact occurs for the α geometry interaction (Figures 3 and 4). We have previously developed a method for studying this interaction by locking the conformation of unsymmetrical complexes with a terminal nitropyrrole group.[9] By using this approach (Figure 6), we can design complexes to hold CX_3–aromatic interactions in the α geometry, thereby ensuring close contact between the halogen and the π system. The proposed double mutant cycles are illustrated in

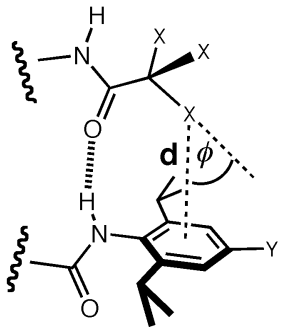

Figure 5. *The α geometry interaction in the X-ray crystal structures of model compounds **4**–**15** is described by the distance between the halogen and the plane of the aromatic ring (d) and the angle between the C–X bond and the plane of the aromatic ring (ϕ).*

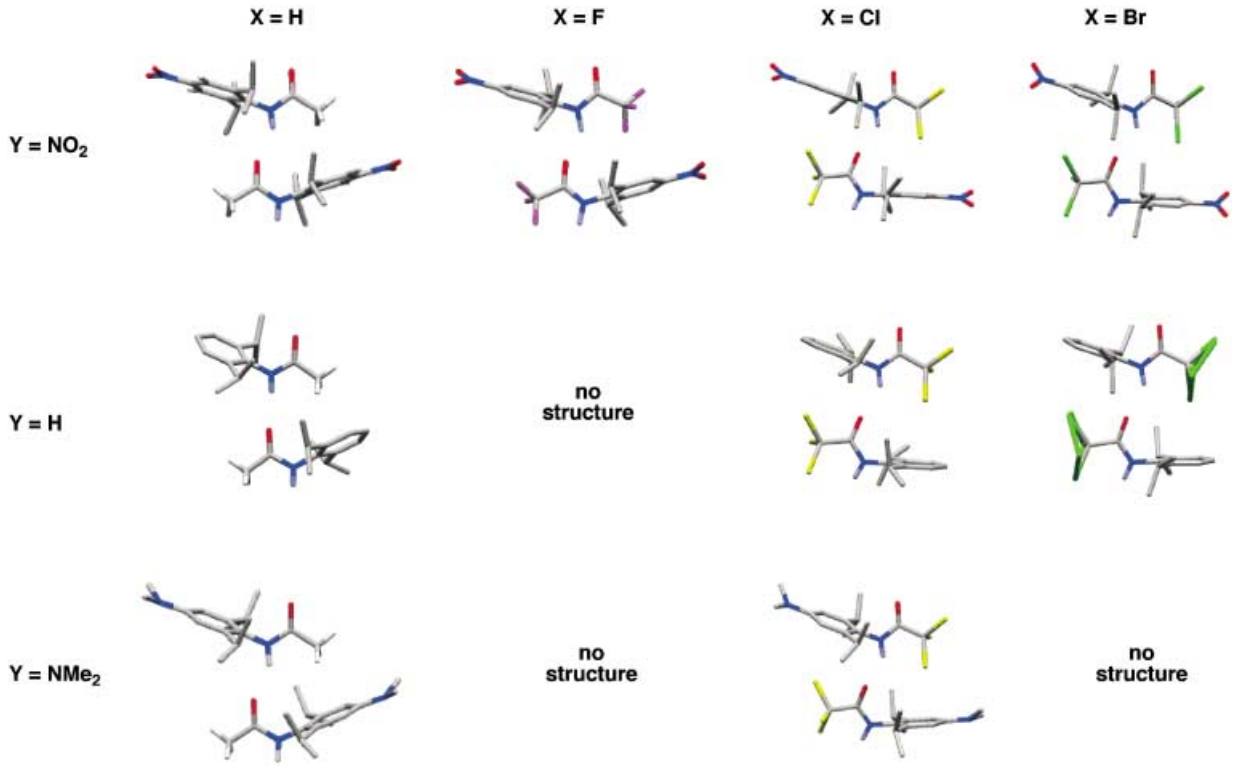

Figure 4. *Dimers found in the X-ray crystal structures of model compounds **4**–**15**. Three compounds (**8**, **9** and **15**) failed to give single crystals suitable for X-ray structure determination. There is some disorder of the CBr_3 group in the structure of compound **14** as illustrated (X = Br, Y = H). Hydrogen atoms are shown in calculated positions. In the structures shown, all compounds pack in a head-to-tail arrangement with hydrogen bonds between the amide groups. The CX_3 groups all lie over the faces of aromatic rings with close halogen–π contacts.*

Table 1. *Geometry of the halogen–aromatic interaction for the closest contact (α geometry) in the X-ray crystal structures of the model compounds shown in Figure 4, and the crystallographic* R *factor for the structures.*[a]

		d [Å]			*ϕ* [°]			*R* [%]		
			X			X			X	
	Y	F	Cl	Br	F	Cl	Br	F	Cl	Br
	NO_2	3.07	3.33	3.61	37	33	33	7	10	9
Y	H	–	3.38	3.38	–	18	35	–	9	6
	NMe_2	–	3.27	–	–	43	–	–	4	–

[a] See Figure 5 for the definition of *d* and *ϕ*.

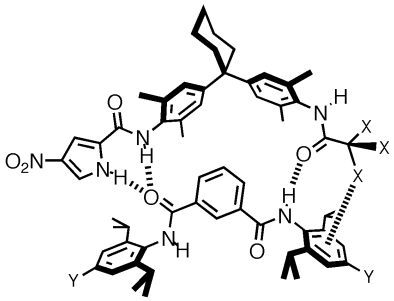

Figure 6. *The complex designed for measuring the halogen–aromatic interaction (X = F, Cl, Br; Y = NO_2, H, NMe_2).*

errors, a simple analysis assuming only 1:1 binding gives double mutant cycle results that are very similar to the results obtained by using a full detailed analysis of all of the equilibria present. For compounds **17**–**20**, low solubility precludes accurate analysis of the competing equilibria, so the data presented are based on the simple 1:1 binding model. The effect of this approximation is to increase the apparent association constants that are reported in Table 2 and increase the size of the errors.

The association constants and limiting complexation-induced changes in chemical shift for the formation of 1:1

Figure 7. Compounds **17**–**19** were therefore synthesised from the known compound **16** (Scheme 2).[9] The other compounds required to construct the required double mutant cycles are shown in Figure 8 and have all been described previously.[7]

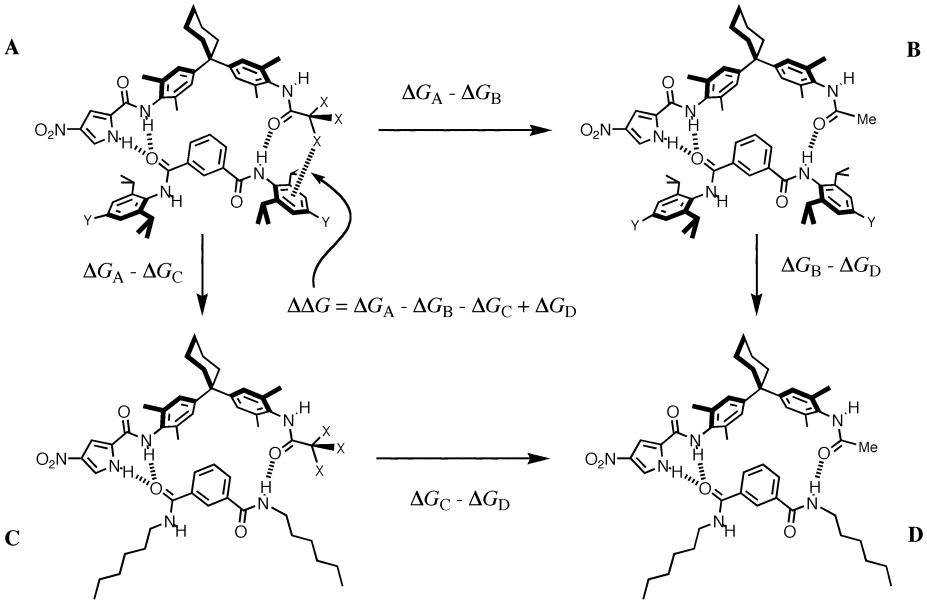

Figure 7. *Chemical double mutant cycle to measure the halogen–aromatic interactions in complex A (X = F, Cl, Br; Y = NO_2, H, NMe_2).*

Binding studies

The complexation properties of the prepared systems were studied by using ^{1}H NMR titration experiments in $CDCl_3$.[7] The behaviour of the bisaniline compounds **17**–**20** is complicated by *cis*–*trans*, *anti*–*syn* conformational equilibria of the amide and nitropyrrole groups, aggregation that takes place with self-association constants of the order of 10 M^{-1}, and low solubility.[9] However, we have shown previously that the errors associated with these equilibria cancel out in the double mutant cycle, and the system behaves well if the bisaniline compounds are used as the guests in the titrations. Thus, although the association constants are subject to significant

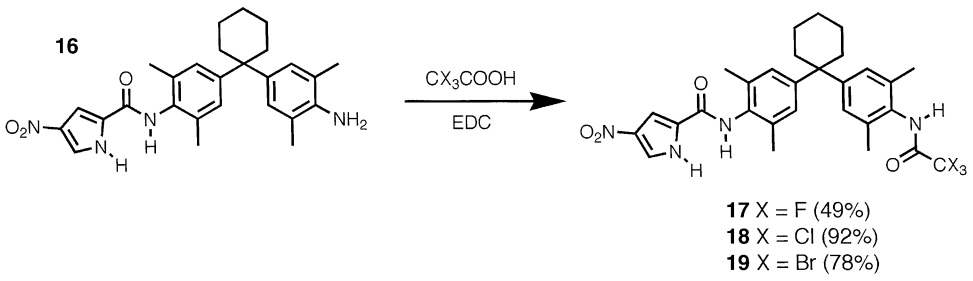

Scheme 2. *Preparation of bisaniline compounds **17**–**20** by direct EDC-mediated coupling of the primary amino function of **16** with the respective trihaloacetic acid.*

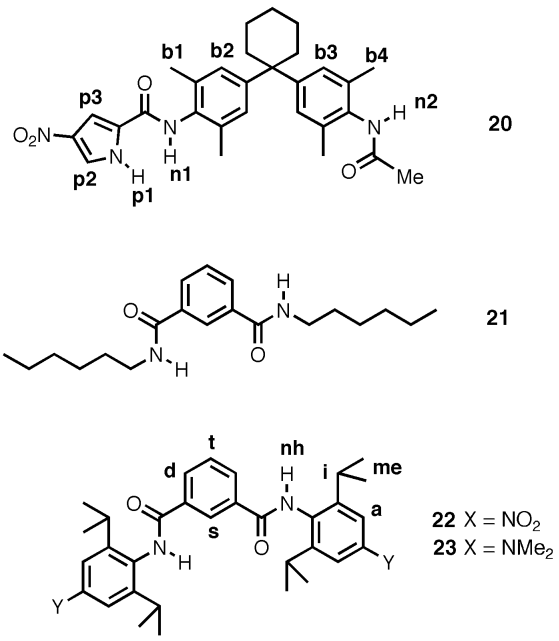

Figure 8. *Compounds used in the double mutant cycles, and the proton labelling scheme.*

complexes are shown in Table 2. Although there are some variations, the pattern of chemical shift changes is similar for all of the complexes indicating that they adopt similar three-dimensional structures in solution.[9,10] There are large downfield shifts of the signals belonging to the pyrrole NH (**p1**), amide **n1** and the isophthaloyl amide (**nh**), and these are indicative of hydrogen-bonding interactions. In most cases, the change in chemical shift for the signal from amide **n2** is much smaller indicating that it is not hydrogen-bonded. For complexes involving **17**, significant increases in chemical shift are observed for **n2**, but this is largely as a result of self-association, which has not been taken into consideration in the analysis of the data. The large consistent upfield shift for the signal belonging to **p2** of the pyrrole indicates that this proton sits over the face of an aromatic ring, so all of the complexes adopt the conformation shown in Figure 6 with the nitropyrrole group locking the orientation of the amides. The large upfield shift observed for the isophthaloyl triplet (**t**) and doublet (**d**) indicate that these protons lie over the face of another aromatic ring. The magnitude of the changes in chemical shift of **d** and **t** are somewhat lower for the complexes involving **22**, which could reflect some difference in the conformation of these complexes. Unfortunately, the low solubility of this compound precludes measurement of the corresponding changes in chemical shift for the bisaniline compound in these complexes. The small downfield shifts observed for the signals belonging to the di-

Table 2. K_a *[M^{-1}] and* ΔG *[kJ mol^{-1}] values and limiting complexation-induced changes in chemical shift (δ in ppm) measured in $CDCl_3$ at 295 K for complexes used in the double mutant cycles.*[a]

					Isophthaloyl compound δ								Bisaniline compound δ							
Complex	Y	X	K_a	ΔG	s	d	t	nh	aa	me	p1	p2	p3	n1	n2	b1	b2	b3	b4	Me
A																				
22·17	NO_2	F	31±5	−8.4±0.4	+0.1	−0.2	−0.5	+0.5	0.0	−0.1	n.d.	n.d.	n.d.	n.d.	n.d.	n.d.	n.d.	n.d.	n.d.	–
2·17	H	F	56±6	−9.9±0.3	+0.1	−0.4	−1.2	+0.6	0.0	−0.1	+0.7	−1.2	0.0	+1.0	+0.7	0.0	+0.1	+0.1	−0.1	–
23·17	NMe_2	F	122±42	−11.8±0.9	+0.2	−0.5	−1.1	+1.3	0.0	−0.1	+1.4	−1.1	+0.1	+1.8	+0.9	0.0	+0.1	+0.1	−0.1	–
22·18	NO_2	Cl	28±6	−8.2±0.6	+0.1	−0.3	−0.8	+0.7	−0.1	−0.1	n.d.	n.d.	n.d.	n.d.	n.d.	n.d.	n.d.	n.d.	n.d.	–
2·18	H	Cl	89±10	−11.0±0.3	+0.3	−0.4	−1.2	+1.2	n.d.	−0.1	+1.2	−1.2	+0.3	+1.8	+0.3	−0.1	+0.1	+0.2	+0.1	–
23·18	NMe_2	Cl	217±42	−13.2±0.5	+0.3	−0.4	−1.2	+1.4	n.d.	−0.1	+1.5	−1.2	+0.1	+1.9	+0.2	−0.1	+0.1	+0.2	+0.1	–
22·19	NO_2	Br	85±39	−10.9±1.1	+0.3	−0.1	−0.3	+1.3	−0.1	−0.1	n.d.	n.d.	n.d.	n.d.	n.d.	n.d.	n.d.	n.d.	n.d.	–
2·19	H	Br	139±26	−12.1±0.5	+0.3	−0.3	−1.0	+1.1	0.0	−0.1	+0.9	−1.1	n.d.	+1.4	+0.1	−0.1	+0.1	+0.2	+0.1	–
23·19	NMe_2	Br	236±44	−13.4±0.5	+0.1	−0.4	−1.2	+0.9	0.0	−0.1	+1.2	−1.1	+0.1	+1.2	+0.1	−0.1	+0.1	+0.2	+0.1	–
B																				
22·20	NO_2	–	104±17	−13.0±0.4	+0.1	−0.2	−0.6	+0.7	0.0	−0.1	n.d.	n.d.	n.d.	n.d.	n.d.	n.d.	n.d.	n.d.	n.d.	n.d.
2·20	H	–	170±40	−12.6±0.6	0.0	−0.4	−1.2	+0.7	0.0	−0.1	+1.3	n.d.	n.d.	+1.9	+0.4	−0.1	+0.2	+0.1	0.0	−0.4
23·20	NMe_2	–	399±98	−14.7±0.6	+0.1	−0.5	−1.3	+0.9	0.0	−0.1	+1.6	−1.2	0.0	+1.9	+0.1	−0.1	+0.1	+0.2	0.0	−0.3
C																				
21·17	–	F	34±3	−8.7±0.3	+0.1	−0.4	−0.8	+0.5	–	–	+1.8	0.0	+0.6	+1.9	+1.7	n.d.	0.0	+0.1	−0.1	–
21·18	–	Cl	32±4	−8.5±0.3	+0.1	−0.4	−0.9	+0.7	–	–	+1.7	0.0	+0.6	+2.0	+0.7	−0.2	−0.1	+0.1	+0.1	–
21·19	–	Br	45±4	−9.3±0.2	+0.1	−0.3	−0.7	+0.6	–	–	+1.3	+0.2	+0.5	+1.7	+0.3	−0.2	−0.1	+0.1	0.0	–
D																				
21·20	–	–	33±8	−8.6±0.6	+0.1	−0.4	−0.8	+0.6	–	–	+1.4	+0.1	+0.6	+1.9	n.d.	0.0	−0.1	+0.1	−0.2	0.0

[a] The data were analysed assuming a simple 1:1 complexation model and ignoring the effects of the conformational and aggregation equilibria that are clearly present in this system. See Figure 8 for the proton labelling scheme. There are no significant changes in chemical shift for the signals belonging to the protons on the cyclohexyl group; n.d. = not determined. Titration experiments were repeated at least twice, and K_a is a weighted mean based on the observed change in chemical shift for all the signals monitored. The error is twice the standard error.

Table 3. *Halogen–aromatic interaction free energies ($\Delta\Delta G$ [kJ mol^{-1}]) measured in $CDCl_3$ at 295 K by using the double mutant cycle shown in Figure 7. Errors are ± 1.0 kJ mol^{-1}.*

		X		
		F	Cl	Br
Y	NO_2	3.0	3.1	1.2
	H	2.8	1.5	1.2
	NMe_2	2.9	1.4	2.0

arylmethane subunit (**b2**–**b4**) indicate that the face of this ring interacts with the edge of another and confirm that edge-to-face aromatic interactions are present in the core of the complex.

The data in Table 2 were used in Equation (1) to construct double mutant cycles for the halogen–aromatic interactions, and the results are shown in Table 3. The interactions are all repulsive. Thus, the interactions that appear to be reliably engineered into the crystal structures of the model compounds reported above are in fact forced there by the neighbouring amide–amide hydrogen bonds and represent contacts that are unfavourable. There are no clear trends in the values of $\Delta\Delta G$ in Table 3, and most of the differences lie within the experimental error. However, the interactions of the aromatic rings with fluorine atoms appear to be slightly more repulsive than with the other halogens.

Conclusion

We have measured noncovalent interactions between a series of halogens and substituted aromatic rings in chloroform. The interactions are all unfavourable, slightly more so for fluorine than for chlorine and bromine. More detailed interpretation of the values is not sensible, as the experiment is subject to a number of limitations:

1) The compounds have low solubility which leads to errors that are large relative to the differences in the interaction energies. All of the results in Table 3 lie within the experimental errors.
2) The complexation-induced changes in chemical shift for the complexes involving **22** (i.e. with the nitro group on the aromatic ring) differ from the rest of the complexes, and may be indicative of a change in conformation for this system.
3) Although the X-ray crystal structures of the model compounds suggest that the supramolecular motif used in these experiments can accommodate all three halogens, the halogens are different in size, and so the observed free energy differences may reflect steric as well as electrostatic effects.
4) The electrostatic potential surfaces of the larger halogens shown in Figure 1 are highly anisotropic, and so relatively subtle changes in geometry could significantly alter the nature of the electrostatic potential surface presented to the π system. The geometry of the zipper complexes is constrained by the architecture of the system, and a different arrangement of the interacting groups could result in quite different interaction energies.

Experimental Section

Synthesis of *N*-(2,6-diisopropyl-4-nitrophenyl)acetamide (4): A solution of 2,6-diisopropyl-4-nitroaniline (0.36 g, 1.6 mmol) and a catalytic amount of 4-(dimethylamino)pyridine (DMAP, 0.04 g) were taken up in anhydrous pyridine (20 mL). Acetyl chloride (0.14 mL, 2.0 mmol) was then added dropwise. The mixture was heated at reflux (140 °C) for 24 h. After this time, the reaction mixture was allowed to cool to room temperature and then poured into 2 M hydrochloric acid cooled on an ice bath. The resulting aqueous mixture was extracted into dichloromethane (2×40 mL). The organic layers were combined, washed with brine and dried over anhydrous sodium sulfate. The solvent was removed under reduced pressure. The main product was the diacetyl derivative, but it was possible to separate the required product in trace amounts (0.01 g, 2%) by column chromatography on silica by using dichloromethane as the eluant. An X-ray crystal structure was used to confirm the structure. ^{1}H NMR (250 MHz, $CDCl_3$): $\delta = 8.05$ (s, 2H), 6.92 (s, 1H), 3.10 (sept, 2H), 2.23 (s, 3H), 1.22 ppm (d, 12H); ^{13}C NMR (250 MHz, $CDCl_3$): $\delta = 170.00$, 148.55, 119.00, 29.26, 26.20, 23.36 ppm.

Synthesis of *N*-(2,6-diisopropylphenyl)acetamide (5): Acetic anhydride (1.5 mL, 5 mmol) was added dropwise to diisopropylaniline (1.1 mL, 5 mmol) in a round-bottomed flask cooled by an ice bath. The resulting solid was filtered and washed sequentially with 1 M hydrochloric acid (2×20 mL), 1 M sodium hydroxide (2×20 mL) and brine (1×20 mL). Recrystallisation from dichloromethane/petroleum ether 40–60 yielded the title compound (12.89 g, 99%) as a white solid. M.p. 198–200 °C; ^{1}H NMR (250 MHz, [D_6]DMSO): $\delta =$ 9.20 (s, 1H), 7.50 (t, 1H), 7.30 (d, 2H), 3.05 (sept, 2H), 1.10 ppm (d, 6H); ^{13}C NMR (250 MHz, [D_6]DMSO): $\delta = 169.48$, 146.40, 133.21, 127.82, 123.25, 28.47, 24.19, 23.69, 22.98 ppm; EIMS: *m/z*: 219 $[M]^+$; elemental analysis calcd (%) for $C_{14}H_{21}NO$: C 76.67, H 9.65, N 6.39; found: C 76.59, H 9.78, N 6.38.

Synthesis of *N*-(2,6-diisopropyl-4-dimethylaminophenyl)acetamide (6): Acetic anhydride (0.046 mL, 0.66 mmol) was added to a stirred solution of 2,6-diisopropyl-4-dimethylaminoaniline (0.09 g, 0.40 mmol) in dry dichloromethane (75 mL) at 0 °C. The temperature was allowed to increase to room temperature. The reaction mixture was washed with 0.5 M sodium hydroxide (4×10 mL) and brine (2×10 mL), and the organic phase was dried over sodium sulfate. Evaporation of the solvent under reduced pressure gave the title compound (0.08 g, 80%) as a brown solid. ^{1}H NMR (250 MHz, $CDCl_3$/[D_6]DMSO): $\delta = 8.79$ (s, 1H), 6.50 (s, 2H), 3.09 (sept, 2H), 2.16 (s, 6H), 1.21 ppm (d, 12H); ^{13}C NMR (250 MHz, $CDCl_3$): $\delta = 170.16$, 150.44, 146.76, 120.91, 107.81, 40.79, 29.02, 24.47, 23.72 ppm; EIMS: *m/z*: 262 $[M]^+$; elemental analysis calcd (%) for $C_{16}H_{26}N_2O$: C 73.24, H 9.99, N 10.68; found: C 73.21, H 10.15, N 10.39.

Synthesis of *N*-(2,6-diisopropyl-4-nitrophenyl)trifluoroacetamide (7): A solution of 2,6-diisopropyl-4-nitroaniline (0.09 g, 0.4 mmol), trifluoroacetic anhydride (0.7 mL, 0.5 mmol) and a catalytic amount of DMAP (0.01 g, 0.07 mmol) were taken up in anhydrous pyridine (10 mL) and heated at reflux (145 °C) for 48 h. After this time, the reaction mixture was allowed to cool to room temperature, and 2 M hydrochloric acid was added gradually until the solution was acidic. The resulting aqueous mixture was extracted into dichloromethane (3×25 mL). The organic layers were combined, washed with brine and dried over anhydrous sodium sulfate. After filtration, the solvent was removed under reduced pressure and the products were separated by column chromatography on silica with dichloromethane/methanol as eluant. The first compound eluted

was the desired product (0.08 g, 60%). ^{1}H NMR (250 MHz, $CDCl_3$): $\delta = 8.09$ (s, 2H), 7.57 (br s, 1H), 3.03 (sept, 2H), 1.26 ppm (d, 12H); ^{13}C NMR (250 MHz, $CDCl_3$): $\delta = 156.15$ (q, $^2J_{CF} = 37$ Hz), 148.70, 148.58, 133.62, 119.34, 116.10 (q, $^1J_{CF} = 286$ Hz), 29.33, 23.24 ppm; ^{19}F NMR ($CDCl_3$): $\delta = -75.50$ ppm; EIMS: *m/z*: 318 $[M]^+$; elemental analysis calcd (%) for $C_{14}H_{17}F_3N_2O_3$: C 52.83, H 5.38, N 8.80; found: C 53.07, H 5.43, N 8.64.

Synthesis of *N*-(2,6-diisopropylphenyl)trifluoroacetamide (8): Trifluoroacetic anhydride (0.75 mL, 5 mmol) was added dropwise to diisopropylaniline (1.1 mL, 5 mmol) in a round-bottomed flask cooled by an ice bath. The resulting solid was filtered and washed with hydrochloric acid (5×20 mL) and brine (1×20 mL). Purification by recrystallisation from dichloromethane/petroleum ether 40–60 yielded the title compound (0.66 g, 46%) as a light pink solid. ^{1}H NMR (250 MHz, [D$_6$]DMSO): $\delta = 9.45$ (s, 1H), 7.25 (t, 1H), 7.15 (d, 2H), 3.02 (sept, 2H), 1.15 ppm (d, 6H); ^{13}C NMR (250 MHz, [D$_6$]DMSO): $\delta = 156.53$ (q, $^2J_{CF} = 36$ Hz), 145.94, 129.87, 129.20, 123.89, 116.70 (q, $^1J_{CF} = 289$ Hz), 28.58, 23.70 ppm; ^{19}F NMR ($CDCl_3$): $\delta = -75.59$ ppm; EIMS: *m/z*: 273 $[M]^+$; elemental analysis calcd (%) for $C_{14}H_{18}F_3NO$: C 61.53, H 6.64, N 5.13; found: C 61.89, H 6.99, N 5.17.

Synthesis of *N*-(2,6-diisopropyl-4-dimethylaminophenyl)trifluoroacetamide (9): Trifluoroacetic anhydride (0.14 g, 0.66 mmol) was added to a stirred solution of 2,6-diisopropyl-4-dimethylaminoaniline (0.11 g, 0.51 mmol) in dry dichloromethane (75 mL). The temperature was allowed to increase to room temperature. The reaction mixture was washed with 0.5 M sodium hydroxide (4×10 mL) and brine (2×10 mL), and the organic phase was dried over sodium sulfate. Evaporation of the solvent under reduced pressure gave the title compound (0.10 g, 62%) as a brown solid. M.p. 196–198 °C; ^{1}H NMR (250 MHz, $CDCl_3$/[D$_6$]DMSO): $\delta = 9.35$ (s, 1H), 6.33 (s, 2H), 2.78 (sept, 2H), 2.78 (s, 6H), 1.00 ppm (d, 12H); ^{13}C NMR (250 MHz, $CDCl_3$): $\delta = 157.16$ (q, $^2J_{CF} = 36$ Hz), 150.99, 146.47, 116.98, 116.30 (q, $^1J_{CF} = 289$ Hz), 107.65, 40.56, 29.08, 23.58 ppm; ^{19}F NMR ($CDCl_3$): $\delta = -75.56$ ppm; HRMS (EI+): *m/z* calcd for $C_{16}H_{23}F_3N_2O$: 316.176; found: 316.176; elemental analysis calcd (%) for $C_{16}H_{23}F_3N_2O$: C 60.75, H 7.33, N 8.85; found: C 60.99, H 7.32, N 8.88.

Synthesis of *N*-(2,6-diisopropyl-4-nitrophenyl)trichloroacetamide (10): A solution of 2,6-diisopropyl-4-nitroaniline (0.36 g, 1.6 mmol), trichloroacetyl chloride (0.18 mL, 2 mmol) and a catalytic amount of DMAP (0.036 g, 0.16 mmol) were taken up in anhydrous pyridine (20 mL) and heated at reflux (145 °C) for 48 h. After this time, the reaction mixture was allowed to cool to room temperature, and 2 M hydrochloric acid was added gradually until the solution was acidic. The resulting aqueous mixture was extracted into dichloromethane (3×25 mL). The organic layers were combined, washed with brine and dried over anhydrous sodium sulfate. After filtration, the solvent was removed under reduced pressure, and crystallisation from chloroform and petroleum ether 40–60 gave the title compound (0.4 g, 66%) as a yellow solid. ^{1}H NMR (250 MHz, $CDCl_3$): $\delta = 8.08$ (s, 1H), 7.90 (s, 1H), 3.15 (sept, 2H), 1.28 ppm (d, 6H); ^{13}C NMR (250 MHz, $CDCl_3$): $\delta = 161.80$, 148.72, 135.08, 119.30, 29.24, 23.28 ppm; CIMS: *m/z*: 384 $[M+NH_3]^+$.

Synthesis of *N*-(2,6-diisopropylphenyl)trichloroacetamide (11): Trichloroacetyl chloride (0.5 mL, 5 mmol) was added to a stirred solution of 2,6-diisopropylaniline (1.1 mL, 5 mmol) and triethylamine (0.7 mL, 5 mmol) in dry dichloromethane (100 mL) in a round-bottomed flask cooled by an ice bath. The temperature was allowed to increase to room temperature. The solvent was evaporated under reduced pressure, and the resulting solid was filtered and washed with hydrochloric acid (5×20 mL) and water (1×20 mL). The desired product was obtained as a light pink solid (1.5 g, 92%). ^{1}H NMR (250 MHz, $CDCl_3$): $\delta = 7.83$ (s, 1H), 7.37 (t, $^1J = 7.8$ Hz, 1H), 7.47 (d, $^1J = 7.8$ Hz, 2H), 3.05 (sept, $^1J = 6.7$ Hz, 2H), 1.25 ppm (d, $^1J = 6.7$ Hz, 6H); ^{13}C NMR (250 MHz, $CDCl_3$): $\delta = 160.99$, 146.26, 129.36, 129.30, 123.83, 28.78, 23.56 ppm; EIMS: *m/z*: 321 $[M]^+$.

Synthesis of *N*-(2,6-diisopropyl-4-dimethylaminophenyl)trichloroacetamide (12): Trichloroacetyl chloride (0.12 g 0.68 mmol) was added to a stirred cold solution of 2,6-diisopropyl-4-dimethylaminoaniline (0.11 g, 0.51 mmol) and triethylamine (0.70 mL, 0.5 mmol) in dry dichloromethane (75 mL). The temperature was allowed to increase to room temperature (RT). The reaction mixture was washed with 0.5 M sodium hydroxide (4×10 mL) and brine (1×10 mL), and the organic phase was dried over sodium sulfate. Evaporation under reduced pressure gave the title compound (0.14 g, 74%) as a brown solid. M.p. 220–222 °C; ^{1}H NMR (250 MHz, $CDCl_3$): $\delta = 7.70$ (s, 1H), 6.50 (s, 2H), 3.00 (sept, 2H), 2.98 (s, 6H), 1.20 ppm (d, 12H); ^{13}C NMR (250 MHz, $CDCl_3$): $\delta = 150.88$, 146.72, 118.57, 107.61, 40.62, 29.01, 23.60 ppm; EIMS: *m/z*: 364 $[M]^+$; elemental analysis calcd (%) for $C_{16}H_{23}Cl_3N_2O$: C 52.55, H 6.34, Cl 29.08, N 7.66; found: C 52.63, H 6.38, Cl 28.88, N 7.41.

Synthesis of *N*-(2,6-diisopropyl-4-nitrophenyl)tribromoacetamide (13): A solution of 2,6-diisopropyl-4-nitroaniline (0.38 g, 1.7 mmol), tribromoacetyl chloride (0.4 mL, 2 mmol) and a catalytic amount of DMAP (0.04 g, 0.17 mmol) were taken up in anhydrous pyridine (20 mL) and heated at reflux (145 °C) for 48 h. After this time, the reaction mixture was allowed to cool to room temperature, and 2 M hydrochloric acid was added gradually until the solution was acidic. The resulting aqueous mixture was extracted into dichloromethane (3×25 mL). The organic layers were combined, washed with brine and dried over anhydrous sodium sulfate. After filtration, the solvent was removed under reduced pressure, and the product was crystallised from chloroform and petroleum ether 40–60. Purification by column chromatography on silica with dichloromethane as eluant gave the title compound (0.31 g, 37%) as a yellow solid. ^{1}H NMR (250 MHz, $CDCl_3$): $\delta = 8.10$ (s, 2H), 7.90 (s, 1H), 3.15 (sept, 2H), 1.25 ppm (d, 6H); ^{13}C NMR (250 MHz, $CDCl_3$): $\delta =$ 148.72, 119.29, 29.21, 23.31 ppm; EIMS: *m/z*: 501 $[M]^+$.

Synthesis of *N*-(2,6-diisopropylphenyl)tribromoacetamide (14): Tribromoacetyl chloride (0.5 mL, 2.6 mmol) was added to a stirred solution of 2,6-diisopropylaniline (0.54 mL, 2.6 mmol) and triethylamine (0.36 mL, 2.6 mmol) in dry dichloromethane (75 mL) on an ice bath. The temperature was allowed to increase to room temperature. The solvent was evaporated under reduced pressure, and the resulting solid was filtered and washed with 1 M hydrochloric acid (5×20 mL) and water (1×20 mL) to afford the title compound (1.05 g, 90%) as a white solid. ^{1}H NMR (250 MHz, $CDCl_3$): $\delta = 8.02$ (s, 1H), 7.35 (t, $^1J = 7.8$ Hz, 1H), 7.20 (d, $^1J = 7.8$ Hz, 2H), 3.10 (sept, $^1J = 6.9$ Hz, 2H), 1.25 ppm (d, $^1J = 6.9$ Hz, 6H); ^{13}C NMR (250 MHz, $CDCl_3$): $\delta = 161.26$, 146.38, 129.59, 129.31, 123.82, 36.51, 28.74, 23.60 ppm; HRMS (FAB+): *m/z* calcd for $C_{14}H_{19}Br_3NO$: 453.902; found: 453.899.

Synthesis of *N*-(2,6-diisopropyl-4-dimethylaminophenyl)tribromoacetamide (15): Tribromoacetyl chloride (0.038 g, 0.32 mmol) was added to a stirred cold solution of 2,6-diisopropyl-4-dimethylaminoaniline (0.068 g, 0.3 mmol) and triethylamine (0.35 mL, 4.7 mmol) in dry dichloromethane (75 mL) at 0 °C. The temperature was allowed to increase to room temperature. The reaction mixture was washed with 0.5 M sodium hydroxide (4×10 mL) and brine (1×10 mL), and the organic phase was dried over sodium sulfate. Evaporation under reduced pressure afforded the title com-

pound (0.18 g, 90%) as a brown solid. ^{1}H NMR (250 MHz, $CDCl_3$): $\delta = 7.87$ (s, 1H), 6.52 (s, 2H), 3.06 (sept, 2H), 2.98 (s, 6H), 1.23 ppm (d, 12H); ^{13}C NMR (250 MHz, $CDCl_3$): $\delta = 161.57$, 150.70, 146.90, 119.89, 107.79, 40.77, 28.97, 23.64 ppm; HRMS (FAB+): *m/z* calcd for $C_{16}H_{24}Br_3N_2O$: 496.944; found: 496.939.

***N*-(4-Nitropyrrole-2-carboxy)-*N'*-trifluoroacetyl-(1,1-bis((4-amino-3,5-dimethyl)phenyl)cyclohexane) (17)**: Trifluoroacetic acid (0.23 mL, 3 mmol) and **16** (0.92 g, 2 mmol) were taken up in dry dichloromethane (150 mL) and cooled to 0°C on an ice bath. After a few minutes, 1-(3-dimethylaminopropyl)-3-ethylcarbodiimide hydrochloride (EDC, 0.57 g, 2.97 mmol) was added to the solution, and the temperature was allowed to increase to room temperature. Purification by recrystallization from dichloromethane/petroleum ether 40–60 gave the title compound (0.55 g, 49%) as a yellow solid. M.p. 188–190°C; ^{1}H NMR (250 MHz, $CDCl_3$/[D$_6$]DMSO): $\delta =$ 11.90 (s, 1H), 9.50 (s, 1H), 8.90 (s, 1H), 7.65 (s, 1H), 7.45 (s, 1H), 6.90 (s, 2H), 6.85 (s, 2H), 2.12 (br s, 4H), 2.08 (s, 6H), 2.05 (s, 6H), 1.40 ppm (br s, 6H); ^{19}F NMR ($CDCl_3$): $\delta = -75.66$ ppm; FABMS: *m/z*; 557 $[M+H]^+$; elemental analysis calcd (%) for $C_{29}H_{31}N_4O_4 \cdot {}^1/_2\,H_2O$: C 61.58, H 5.70, N 9.91; found: C 61.75, H 5.67, N 9.64.

***N*-(4-Nitropyrrole-2-carboxy)-*N'*-trichloroacetyl-(1,1-bis((4-amino-3,5-dimethyl)phenyl)cyclohexane) (18)**: Trichloroacetic acid (0.40 g, 2.45 mmol) and **16** (0.83 g, 1.8 mmol) were taken up in dry dichloromethane (150 mL) and cooled to 0°C on an ice bath. After a few minutes, EDC (0.6 g, 3.0 mmol) was added to the solution, and the temperature was allowed to increase to room temperature. The product was purified by washing with 1 M hydrochloric acid (4×15 mL) and 1 M sodium hydroxide (4×15 mL). The organic solution was dried over anhydrous sodium sulfate, and the solvent was evaporated under reduced pressure to give the title compound (0.83 g, 92%) as a yellow solid. M.p. 167–169°C; ^{1}H NMR (250 MHz, $CDCl_3$): $\delta = 9.80$ (s, 1H), 7.82 (s, 1H), 7.78 (dd, $^1J = 3.4$, $^2J = 1.4$ Hz, 1H), 7.23 (dd, $^2J = 2.4$, $^2J = 1.4$ Hz, 1H), 7.11 (s, 1H), 7.01 (s, 2H), 7.00 (s, 2H), 2.23 (s, 6H), 2.21 (s, 6H), 2.20 (br s, 4H), 1.54 ppm (br s, 6H); ^{13}C NMR (250 MHz, $CDCl_3$/[D$_6$]DMSO): $\delta =$ 160.42, 158.53, 148.18, 147.20, 137.13, 135.39, 135.19, 131.10, 129.95, 126.82, 126.47, 126.50, 122.00, 106.20, 45.22, 36.54, 26.19, 22.78, 18.79, 18.27 ppm; FABMS: *m/z*: 607 $[M+H]^+$.

***N*-(4-Nitropyrrole-2-carboxy)-*N'*-tribromoacetyl-(1,1-bis((4-amino-3,5-dimethyl)phenyl)cyclohexane) (19)**: Tribromoacetic acid (0.85 g, 2.8 mmol) and **16** (1.09 g, 2.4 mmol) were taken up in dry dichloromethane (150 mL) and cooled to 0°C by using an ice bath. After a few minutes, EDC (0.64 g, 3.3 mmol) was added to the solution, and the temperature was allowed to increase to room temperature. The solution was washed with 1 M hydrochloric acid (3× 15 mL) and 1 M sodium hydroxide (3×15 mL). The solvent was evaporated under reduced pressure, and the brown solid was purified by recrystallization from dichloromethane/petroleum ether 40–60 to afford the title compound (1.37 g, 78%). M.p. 205–206°C; ^{1}H NMR (250 MHz, $CDCl_3$): $\delta = 10.28$ (s, 1H), 8.03 (s, 1H), 7.77 (dd, $^1J = 3.5$, $^2J = 1.4$ Hz, 1H), 7.25 (dd, $^2J = 2.4$, $^2J = 1.4$ Hz, 1H), 7.12 (s, 1H), 7.01 (s, 2H), 7.00 (s, 2H), 2.25 (s, 6H), 2.20 (s, 6H), 2.20 (br s, 4H), 1.54 ppm (br s, 6H); ^{13}C NMR (250 MHz, $CDCl_3$): $\delta =$ 160.70, 158.73, 148.27, 147.96, 137.46, 135.34, 135.25, 130.36, 129.74, 127.15, 126.82, 125.76, 122.00, 105.92, 45.27, 36.80, 30.94, 26.24, 22.85, 18.79, 18.40 ppm; HRMS: *m/z* calcd for $C_{26}H_{32}Br_3N_4O_4$: 736.997; found: 736.990.

Crystal structure data: CCDC-229124 to 229132 contain the supplementary crystallographic data for this paper. These data can be obtained free of charge via www.ccdc.cam.ac.uk/conts/retrieving.html (or from the Cambridge Crystallographic Data Centre, 12 Union Road, Cambridge CB2 1EZ, UK; fax: (+44) 1223-336033; or deposit@ccdc.cam.uk).

Compound 4: Crystal data for $C_{14}H_{20}N_2O_3$: $M_r = 264.32$; crystallises from methanol as light brown blocks; crystal dimensions 0.32× 0.12×0.12 mm. Orthorhombic, $a = 9.1715(18)$, $b = 10.738(2)$, $c =$ 15.152(3) Å, $U = 1492.1(5)$ Å^3, $Z = 4$, $\rho_{calcd} = 1.177$ Mg m^{-3}, space group *Pnma* (D_{2h}^{16}, No.62, $Mo_{K\alpha}$ radiation ($\lambda = 0.71073$ Å), $\mu(Mo_{K\alpha}) =$ 0.083 mm^{-1}, $F(000) = 568$.

Compound 5: Crystal data for $C_{14}H_{21}NO$: $M_r = 219.32$; crystallises from dichloromethane/petroleum ether as colourless blocks; crystal dimensions 0.55×0.27×0.25 mm. Orthorhombic, $a = 17.799(7)$, $b = 8.492(3)$, $c = 9.326(5)$ Å, $U = 1409.6(11)$ Å^3, $Z = 4$, $\rho_{calcd} =$ 1.033 Mg m^{-3}, space group $Pca2_1$ (C_2^5, No.29), $Mo_{K\alpha}$ radiation ($\lambda =$ 0.71073 Å), $\mu(Mo_{K\alpha}) = 0.064$ mm^{-1}, $F(000) = 480$.

Compound 6: Crystal data for $C_{16}H_{26}N_2O$: $M_r = 262.39$, crystallises from methanol as colourless plates; crystal dimensions 0.41× 0.21×0.12 mm. Monoclinic, $a = 16.181(2)$, $b = 10.5392(16)$, $c =$ 9.3966(14) Å, $\beta = 90.000(3)°$, $U = 1602.4(4)$ Å^3, $Z = 4$, $\rho_{calcd} =$ 1.088 Mg m^{-3}, space group $P2_1/c$ (C_{2h}^5, No.14), $Mo_{K\alpha}$ radiation ($\lambda =$ 0.71073 Å), $\mu(Mo_{K\alpha}) = 0.068$ mm^{-1}, $F(000) = 576$.

Compound 7: Crystal data for $C_{14}H_{17}F_3N_2O_3$: $M_r = 318.50$; crystallises from dichloromethane as colourless plates; crystal dimensions 0.30×0.30×0.12 mm. Orthorhombic, $a = 9.43(4)$ $b = 10.51(4)$, $c =$ 15.89(6) Å, $U = 1574(11)$ Å^3, $Z = 4$, $\rho_{calcd} = 1.343$ Mg m^{-3}, space group $P2_12_12_1$ (D_2^4, No.19), $Mo_{K\alpha}$ radiation ($\lambda = 0.71073$ Å), $\mu(Mo_{K\alpha}) =$ 0.118 mm^{-1}, $F(000) = 664$.

Compound 10: Crystal data for $C_{14}H_{17}Cl_3N_2O_3$: $Mr = 367.65$; crystallises from dichloromethane as colourless needles; crystal dimensions 0.21×0.12×0.12 mm. Monoclinic, $a = 10.84(3)$, $b = 16.75(4)$, $c =$ 9.76(2) Å, $\beta = 97.96(2)°$, $U = 1755(7)$ Å^3, $Z = 4$, $\rho_{calcd} = 1.392$ Mg m^{-3}, space group $P2_1/c$ (C_{2h}^5, No.14), $Mo_{K\alpha}$ radiation ($\lambda = 0.71073$ Å), $\mu(Mo_{K\alpha}) = 0.534$ mm^{-1}, $F(000) = 760$.

Compound 11: Crystal data for $C_{14}H_{18}Cl_3NO$: $M_r = 322.64$; crystallises from dichloromethane as colourless needles; crystal dimensions 0.21×0.08×0.08 mm. Monoclinic, $a = 10.145(3)$, $b = 17.913(5)$, $c =$ 9.847(3) Å, $\beta = 116.012(6)°$, $U = 1608.1(8)$ Å^3, $Z = 4$, $\rho_{calcd} =$ 1.333 Mg m^{-3}, space group $P2_1/c$ (C_{2h}^5, No.14), $Mo_{K\alpha}$ radiation ($\lambda =$ 0.71073 Å), $\mu(Mo_{K\alpha}) = 0.562$ mm^{-1}, $F(000) = 672$.

Compound 12: Crystal data for $C_{16}H_{23}Cl_3N_2O$: $M_r = 365.71$; crystallises from dichloromethane as colourless needles; crystal dimensions 0.21×0.12×0.12 mm. Monoclinic, $a = 9.6323(8)$, $b = 9.6702(8)$, $c =$ 20.5301(18) Å, $\beta = 97.741(2)°$, $U = 1894.9(3)$ Å^3, $Z = 4$, $\rho_{calcd} =$ 1.282 Mg m^{-3}, space group $P2_1/c$ (C_{2h}^5, No.14), $Mo_{K\alpha}$ radiation ($\lambda =$ 0.71073 Å), $\mu(Mo_{K\alpha}) = 0.486$ mm^{-1}, $F(000) = 768$.

Compound 13: Crystal data for $C_{14}H_{17}Br_3N_2O_3$: $M_r = 501.03$; crystallises from chloroform/petroleum ether as colourless blocks; crystal dimensions 0.13×0.11×0.06 mm^3. Monoclinic, $a = 9.769(2)$, $b =$ 16.817(3), $c = 10.820(2)$ Å, $\beta = 99.26(3)°$, $U = 1754.5(6)$ Å^3, $Z = 4$, $\rho_{calcd} = 1.897$ Mg m^{-3}, space group $P2_1/c$ (C_{2h}^5, No.14), $Mo_{K\alpha}$ radiation ($\lambda = 0.71073$ Å), $\mu(Mo_{K\alpha}) = 6.910$ mm^{-1}, $F(000) = 976$.

Compound 14: Crystal data for $C_{14}H_{18}Br_3NO$: $M_r = 456.02$; crystallises from acetone/petroleum ether as colourless blocks; crystal dimensions 0.30×0.20×0.12 mm. Monoclinic, $a = 10.270(3)$, $b =$ 18.254(6), $c = 9.994(3)$ Å, $\beta = 117.350(6)°$, $U = 1664.1(10)$ Å^3, $Z = 4$, $\rho_{calcd} = 1.820$ Mg m^{-3}, space group $P2_1/c$ (C_{2h}^5, No.14), $Mo_{K\alpha}$ radiation ($\lambda = 0.71073$ Å), $\mu(Mo_{K\alpha}) = 7.265$ mm^{-1}, $F(000) = 888$.

Acknowledgements

We thank the Lister Institute (C.A.H.), EPSRC (J.P.), AstraZeneca (C.G.), Zeneca Agrochemicals (J.P.) and Hoffman–La Roche (S.L.C.) for financial support.

Keywords: double mutant cycles · halogens · hydrogen bonds · molecular recognition · pi interactions

[1] a) K. Yamasaki, *J. Phys. Soc. Jpn.* **1962**, *17*, 1264; b) S. C. Nyburg, *J. Chem. Phys.* **1962**, *48*, 4890; c) D. H. Rank, B. S. Rao, *J. Mol. Spect.* **1964**, *13*, 34–42; d) O. Hassel, J. Hvoslef, J. *Science* **1970**, *170*, 497–502; e) K. Mirsky, M. D. Cohen, *Chem. Phys.* **1978**, *28*, 193–204; f) L.-Y. Hsu, D. E. Williams, *Inorg. Chem.* **1979**, *18*, 79–82; g) S. C. Nyburg, W. Wong-Ng, *Proc. Royal Soc. London Ser. A* **1979**, *367*, 29–45; h) S. C. Nyburg, W. Wong-Ng, *Inorg. Chem.* **1979**, *18*, 2790–2791; i) L.-Y. Hsu, D. E. Williams, *Inorg. Chem.* **1980**, *19*, 2200; j) E. Burgos, C. S. Murthy, R. Righini, *Mol. Phys.* **1982**, *47*, 1391–1403; k) S. L. Price, A. J. Stone, J. Lucas, R. S. Rowland, A. E. Thornley, *J. Am. Chem. Soc.* **1994**, *116*, 4910–4918; l) H. I. Bloemink, K. Hinds, A. C. Legon, J. C. Thorn, *Angew. Chem.* **1994**, *106*, 1577–1579; *Angew. Chem. Int. Ed. Engl.* **1994**, *33*, 1512–1513; m) D. E. Williams, G. Daquan, *Inorg. Chem.* **1997**, *36*, 782–788; n) V. Amico, S. V. Meille, E. Corradi, M. T. Messina, G. Resnati, *J. Am. Chem. Soc.* **1998**, *120*, 8261; o) A. Lunghi, P. Cardillo, M. T. Messina, P. Metrangolo, W. Panzeri, G. Resnati, *J. Fluor. Chem.* **1998**, *91*, 191; p) J. M. A. Robinson, B. M. Kariuki, K. D. M. Harris, D. Philp, *J. Chem. Soc. Perkin Trans. 2* **1998**, 2459–2469; q) E. Corradi, S. V. Meille, M. T. Messina, P. Metrangolo, G. Resnati, *Angew. Chem.* **2000**, *112*, 1852–1856; *Angew. Chem. Int. Ed.* **2000**, *39*, 1782–1786.

[2] a) O. Hassel, J. Hvoslef, *Acta Chem. Scand.* **1954**, *8*, 873; b) O. Hassel, J. Hvoslef, *Proc. Chem. Soc.* **1957**, 250.

[3] S. L. Price, A. J. Stone, *Mol. Phys.* **1982**, *47*, 1457–1470.

[4] a) P. Murray-Rust, W. D. S. Motherwell, *J. Am. Chem. Soc.* **1979**, *101*, 4374–4376; b) V. R. Pedireddi, S. D. Reddy, B. S. Gould, D. C. Craig, A. D. Rae, G. R. Desiraju, *J. Chem. Soc. Perkin Trans. 2* **1994**, 2353–2360; c) J. P. M. Lommerse, A. J. Stone, R. Taylor, F. H. Allen, *J. Am. Chem. Soc.* **1996**, *118*, 3108–3116; d) F. H. Allen, *Acta Crystallogr. B* **1997**, *53*, 1006–1016; e) M. D. Prasanna, T. N. G. Row, *Cryst. Eng.* **2000**, *3*, 135–154.

[5] a) R. S. Mulliken, *J. Am. Chem. Soc.* **1950**, *72*, 600–608; b) J. L. Lippert, M. W. Hanna, P. J. Trotter, *J. Am. Chem. Soc.* **1969**, *91*, 4035–4044.

[6] Y. Nakai, G. Yamamoto, M. Ooki, *Chem. Lett.* **1987**, 89–92.

[7] a) H. Adams, F. J. Carver, C. A. Hunter, J. C. Morales, E. M. Seward, *Angew. Chem.* **1996**, *108*, 1628–1631; *Angew. Chem. Int. Ed. Engl.* **1996**, *35*, 1542–1544; b) H. Adams, K. D. M. Harris, G. A. Hembury, C. A. Hunter, D. Livingstone, J. F. McCabe, *Chem. Commun.* **1996**, 2531–2532; c) F. J. Carver, C. A. Hunter, E. M. Seward, *Chem. Commun.* **1998**, 775–776; d) G. Chessari, C. A. Hunter, J. L. Jiminez Blanco, C. M. R. Low, J. G. Vinter in *NMR in Supramolecular Chemistry* (Ed.: M. Pons), Kluwer, **1999**, 331–334; e) F. J. Carver, C. A. Hunter, P. S. Jones, D. J. Livingstone, J. F. McCabe, E. M. Seward, P. Tiger, *Chem. Eur. J.* **2001**, *7*, 4854–4862; f) H. Adams, J.-L. Jiminez Blanco, G. Chessari, C. A. Hunter, C. M. R. Low, J. M. Sanderson, J. G. Vinter, *Chem. Eur. J.* **2001**, *7*, 3494–3503; g) F. J. Carver, C. A. Hunter, D. J. Livingstone, J. F. McCabe, E. M. Seward, *Chem. Eur. J.* **2002**, *8*, 2848–2859; h) C. A. Hunter, P. S. Jones, P. Tiger, S. Tomas, *Chem. Eur. J.* **2002**, *8*, 5435–5446; i) C. A. Hunter, C. M. R. Low, C. Rotger, J. G. Vinter, C. Zonta, *Proc. Natl. Acad. Sci. USA* **2002**, *99*, 4873–4876; j) C. A. Hunter, C. M. R. Low, C. Rotger, J. G. Vinter, C. Zonta, *Chem. Commun.* **2003**, 834–835; k) C. A. Hunter, C. M. R. Low, J. G. Vinter, C. Zonta, *J. Am. Chem. Soc.* **2003**, *125*, 9936–9937.

[8] H. Adams, P. L. Bernad, D. S. Eggleston, R. C. Haltiwanger, K. D. M. Harris, G. A. Hembury, C. A. Hunter, D. J. Livingstone, B. M. Kariuki, J. F. McCabe, *Chem. Commun.* **2001**, 1500–1501.

[9] H. Adams, C. A. Hunter, K. R. Lawson, J. Perkins, S. E. Spey, C. J. Urch, J. M. Sanderson, *Chem. Eur. J.* **2001**, *7*, 4863–4877.

[10] C. A. Hunter, M. J. Packer, *Chem. Eur. J.* **1999**, *5*, 1891–1897.

Received: January 20, 2004 [F400018]

